Chapter 1

INTRODUCTION

Almost twenty years ago, the spontaneous formation of pillars from a molten nanofilm in a confined geometry subject to a transverse thermal gradient was observed by Chou and Zhuang [2, 3]. In their experiment, solid polymeric nanofilms were spun coat on a silicon wafer with an initial film thickness, h_o, of approximately one hundred nanometers. Subsequently, another silicon wafer was overlaid on this coated wafer. To ensure an air gap between the top surface of the nanofilm and the overlaid wafer, the wafer was patterned with spacers which determined the total plate separation distance, d_o, and this distance was typically on the order of several hundred nanometers to a micron. A schematic of their experimental setup is shown in Fig. 1.1. Upon heating, the temperature of the system was raised significantly above the glass transition temperature so that the film was in a molten state. After deformation times ranging from 5 to 80 minutes, the molten film was allowed to solidify and hexagonal arrays of pillars with lateral spacing on the order of microns were observed after the bounding plate was removed. These pillars had spanned the air gap during deformation and contacted the top plate, creating pillars with flat tops and fairly vertical sidewalls. At the time, there was no explanation for this phenomenon. It has since generated controversy over the dominant physical mechanism that causes the molten nanofilm to be unstable in this system. Several possibilities have been put forth and will be discussed in turn.

Figure 1.1: Basic nanofilm instability geometry

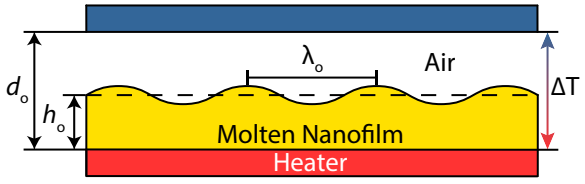

Schematic of the nanofilm geometry. The molten nanofilm is bounded from below by a heated substrate and from above by an air layer. The air layer is bounded from above by a plate where the total plate separation, d_o, is typically on the order of a micron, while the initial film thickness, h_o, is on the order of hundreds of nanometers. The temperature drop from bottom to top plates is typically on the order of 10 °C. The lateral spacing of the protrusions, λ_o, is on the order of microns to tens of microns.

1.1 Previous Instability Investigations: Surface Charge (SC) Model

The first model proposed to explain the instability of this film was put forward by Chou and Zhuang [2, 3]. Their model treats the molten nanofilm from the perspective of fluid dynamics wherein it is linearly unstable to perturbations. They hypothesized that charges at the nanofilm's free interface induce image charges in the heating and cooling plates. The combined effect of these charges creates an electric field which exerts a destabilizing electrostatic stress on the interface to overcome the stabilizing force of surface tension. Due to its dependence on interfacial charge density, this model will be referred to as the surface charge (SC) model. Interestingly, they noted that in addition to electrical effects, thermal effects might be playing a role because if the molten nanofilm was not bounded from above by the overlaid wafer, then the pillars were not observed after solidification of the film. However, they did not intentionally impose a thermal gradient across the system with active cooling of the top plate. Additionally, they estimated that the critical numbers for cellular convection driven by thermal effects such as Rayleigh-Bénard and Bénard-Marangoni convection were far too small for instability to occur. Regardless, the spatial period of the observed hexagonal arrays showed an unexplained dependence on the temperature of the system.

1.2 Previous Instability Investigations: Acoustic Phonon (AP) Model

Nearly simultaneously with the work of Chou and Zhuang, Schäffer and co-workers investigated an instability in a similar geometry [4–6]. As before, they spun coat polymeric nanofilms onto silicon substrates and placed them in a confined geometry through the use of spacers. The key difference from the experiments of Chou and Zhuang is that in the experiments of Schäffer *et al.* the top plate was actively cooled. The cooler top plate was held at a temperature above the glass transition temperature of the polymer and the temperature difference between the bounding plates was on the order of 10 °C. The setup was subjected to this externally imposed transverse thermal gradient overnight and then the nanofilm was solidified. Once again, hexagonal arrays of pillars with flat tops were observed upon removal of the top plate. To rule out any electrostatic effects, both of the bounding plates were electrically grounded. As Chou and Zhuang did, Schäffer *et al.* calculated the Rayleigh-Bénard and Bénard-Marangoni numbers in nanofilm experiments and found that they were many orders of magnitude smaller than the critical ones required for instability. To explain the observed results, they suggested that the instability might be due to an acoustic phonon mechanism leading to periodic modulation of the acoustic pressure

within the film. In this model, acoustic phonon reflections create a net acoustic pressure which destabilizes the interface and causes protrusions to grow. Specifically, they conjectured that phonons with low frequency would be coherently reflected off the nanofilm/air interface while high frequency phonons would be unaffected by the interface and conduct most of the heat flux through the system. These low frequency phonon reflections would then contribute a significant destabilizing radiation pressure which overpowers surface tension to create protrusions. This model will be referred to as the acoustic phonon (AP) model.

Following a derivation of a complete hydrodynamic theory describing the instability in terms of the radiation pressure, they used linear stability analysis to derive a result for the characteristic spacing of the film's fastest growing mode, λ_o, as a function of the initial film thickness, h_o, total plate separation, d_o, and temperature drop, ΔT. They then performed a set of experiments to probe the functional dependence of λ_o on d_o by introducing a tilt between the bottom and top plates to measure a range of d_o for a single run at a given h_o value. They repeated this procedure for several values of h_o. By fitting one of the parameters in their theory, they were able to find agreement between the experimental data and the theoretical prediction for λ_o over a limited range of d_o. Due to their decision to vary d_o through substrate tilt, they were only able to measure values of d_o that varied by a factor of three in a given experimental run and only achieved a range of a factor of six over all the experimental runs. Furthermore, the induced substrate tilt induced an extra lateral gradient which was not included in their model. More problematic for their comparisons to the wavelength predicted by linear stability theory, the values that they reported for λ_o were all measured far outside of the linear regime because the deformations were allowed to contact the top plate and solidify. Prolonged contact with the top plate can drastically changed the pattern morphology through coarsening or van der Waals interactions which were not considered in the AP model. Furthermore, several measurements were made in regions where growth of structures was nucleated by defects which would also invalidate the comparison of the experimental data to linear stability theory.

Following in this vein, Peng *et al.* demonstrated formation of hexagonal arrays from heated polymeric nanofilms in confined geometries [7], similar to what had been previously reported by Schäffer *et al.*. They then took the hexagonal patterns and transferred them to a stamp made of polydimethylsiloxane (PDMS) which could then be used for future microfabrication steps. Even though there was strong ordering in

these systems, Peng *et al.* did not measure the spacing of their arrays as a function of h_o, d_o, or ΔT, nor did they compare to any proposed model.

1.3 Previous Instability Investigations: Thermocapillary (TC) Model

Several years later, Dietzel and Troian began to investigate these issues and re-evaluated the assumptions of the SC and AP models [8–10]. In particular, they noted that phonon mean free paths on the order of ten to one hundred nanometers required for coherent reflection from the film interface in the AP model have only been measured in solid polymer systems at temperatures far below the glass transition temperature. They conclude that it is unlikely that molten amorphous films would be able to support the long attenuation lengths due to the increased mobility of the polymeric system above the glass transition temperature. They also reexamined the assertion by both Chou *et al.* [2] and Schäffer *et al.* [6] that the critical numbers which typically govern Bénard-Marangoni convection would be too small in nanofilm experiments for instability. Their theoretical and computational work [8–10] has indicated that the instability represents a new limit of the long wavelength Bénard-Marangoni instability, distinguished by extremely large thermocapillary forces and negligible hydrostatic forces, which is not governed by the traditional critical numbers. The underlying concept for this model is that protrusions will be slightly cooler than valleys and they will have a correspondingly higher surface tension. This gradient in surface tension between peaks and valleys creates a destabilizing shear stress along the interface which causes lateral flow and, through incompressibility, out of plane protrusion growth. This model will be referred to as the thermocapillary (TC) model. Based on the TC model, they also derived a prediction for the characteristic spacing of the film's fastest growing mode, λ_o, as a function of the initial film thickness, h_o, total plate separation, d_o, and temperature drop, ΔT, and compared it to the experimental data of Schäffer *et al.* [4–6] and concluded that the TC model was consistent with the experimental data to that point, and could potentially play a critical, if not dominant, role in the film evolution.

Shortly thereafter, McLeod *et al.* performed a series of experimental wavelength measurements to further investigate the underlying instability mechanism [1]. These experiments focused on improving the experimental measurement techniques to more accurately compare the measured wavelengths to the predictions of linear stability theory from the SC, AP, and TC models. In particular, they performed *in situ* optical measurements of the instability during the deformation process to

measure λ_o when the deformations were small compared to the initial film thickness and well before the protrusions contacted the top plate. Furthermore, none of the previous experiments had measured or calculated the temperature drop across the nanofilm/air bilayer. Due to the minute size of the gap, it is impossible to directly measure the temperature in the gap using a thermocouple. Instead, the difference between heater and chiller setpoints was taken to be equal to the temperature drop across the bilayer. McLeod *et al.* improved upon this procedure by performing finite element simulations of the experimental setup based on thermocouple measurements to compute the temperature difference across the bilayer. They also performed many more experimental runs than Schäffer *et al.* [4–6] and swept a much larger range of d_o, h_o, and ΔT. With this experimental setup, they found that the experimental data for the measured wavelength was most consistent with the TC model, but that close numerical agreement required the thermal conductivity of the polymer nanofilm to be fit. The required value for the vertical, out-of-plane polymer thermal conductivity was found to be five times larger than the bulk value. It was originally postulated that polymer chain alignment could account for the increase in thermal conductivity, but this hypothesis is problematic for two reasons. First, in cases where polymer alignment has been observed [11], the polymer used was well above the entanglement molecular weight where long chains can interact. Conversely, the polymer used in the work of McLeod *et al.* was well below the entanglement limit so a potential alignment mechanism is not clear. Second, the increase in thermal conductivity of spin coated polymeric thin films has been observed in the lateral direction, not the vertical one [12]. As such, even with the improved experimental setup, there remained discrepancies between the experimental measurements and the theoretical predictions.

1.4 Pattern Replication through Controlled Film Deformation

Concurrently with the fundamental science investigations into the underlying instability mechanism presented above, there has been research into controlling and localizing feature deformation as a potential manufacturing technique. To do this, the locally flat top plate from Fig. 1.1 was patterned with another set of features which stretch toward the nanofilm in addition to the spacers. A schematic of this geometry is shown in Fig. 1.2. In all three models, the presence of a patterned mask on the top plate will localize deformation and allow for control of the film because the mask changes the local gap width.

The first demonstration of pattern replication in these types of geometries was by

Figure 1.2: Basic nanofilm deformation geometry with a patterned top plate

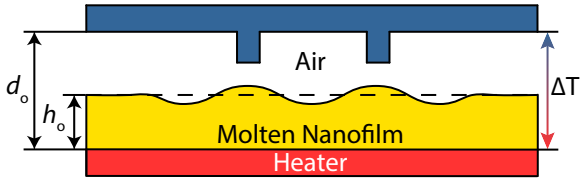

Schematic of the nanofilm geometry where the feature deformation is localized by patterns on the top plate. The ranges for the experimental parameters are the same as for Fig. 1.1.

Chou and co-workers where they patterned the top plate with a triangle, a square and the text "PRINCETON" [2, 13]. In each case, they observed pillar arrays in the shape of the patterned mask and virtually no deformation in the regions outside the mask. In a related study, Chou *et al.* observed that the film would completely cover the applied mask if it was closer in proximity to the initial film height [14]. In this case, the pillar arrays merged into a continuous feature which replicated the mask. Similarly, Schäffer *et al.* demonstrated pattern replication of hexagonal arrays, square arrays, and lines with feature sizes as small as 500 nm [4, 15]. In all of the cases just discussed, the features were allowed to grow until they contacted the mask. This meant that all the features had flat tops due to their interaction with the mask. Instead of allowing the film to grow unchecked, McLeod and Troian stopped the film deformation before it interacted with the mask to produce a square array of curved lenses [16]. This experimental work corresponds more closely with the schematic in Fig. 1.2 than the previous studies which would have touched the mask protrusions. The ability to localize nanofilm deformations using patterned masks opens up a new avenue for the fabrication of unique structures with ultrasmooth surfaces. This system profiles as a novel lithographic technique, but more work needs to be done to understand the advantages and limitations.

1.5 Thesis Outline

In the spirit of the previous studies mentioned above, this thesis seeks to investigate and understand the residual discrepancies between the experimental instability data and the theoretical predictions. It also seeks to deform nanofilms into structures through the use of patterned masks on the top plate and then characterize their properties. As such, the remainder of this thesis is organized as follows. In Ch. 2, the equations describing the distinct sources of instability proposed to explain the spontaneous nanofilm deformation are reviewed. For each of the three previously proposed linear instability models (SC, AP, and TC), predictions for the fastest

growing mode and its corresponding wavelength and growth rate are compared. The next three chapters focus on the experimental and numerical work which investigated the dominant physical mechanism driving this thin film instability. Specifically, in Ch. 3 improved analysis techniques for image analysis and thermal simulation are detailed to improve the comparison of measured wavelengths to the AP and TC models. In Ch. 4 the growth of protrusions are measured as a function of time using colorimetric information derived from thin film interference fringes. The resulting growth rates are compared to the predictions of the TC model. Next, an improved experimental setup is detailed and the instability measurements which were made with it are described in Ch. 5. The results of these experiments strongly indicate that the dominant instability mechanism is caused by interfacial thermocapillary stresses. After this, the next two chapters focus on the fabrication of two kinds of micro-optical components using thermocapillary forces. First, microlens arrays were fabricated and characterized. The results of this study are presented in Ch. 6. Beyond microlens arrays, linear optical waveguides were also fabricated and characterized and this work is described in Ch. 7. Finally, Ch. 8 describes conclusions from the thesis and suggests experimental improvements for future studies.